The Astrophysical Journal, 569:1009–1015, 2002 April 20

SOLAR PHENOMENA ASSOCIATED WITH "EIT WAVES"

D. A. Biesecker and D. C. Myers
Emergent Information Technologies, Inc., NASA Goddard Space Flight Center, Mail Code 682.3, Greenbelt, MD 20771;
doug@sungrazer.nascom.nasa.gov, dcm@chippewa.nascom.nasa.gov

B. J. Thompson
NASA Goddard Space Flight Center, Mail Code 682.3, Greenbelt, MD 20771; thompson@eitv3.nascom.nasa.gov

D. M. Hammer
Emergent Information Technologies, Inc., NASA Goddard Space Flight Center, Mail Code 682.3, Greenbelt, MD 20771;
derek@sungrazer.nascom.nasa.gov

and

A. Vourlidas
George Mason University, E. O. Hulburt Center for Space Research, Naval Research Laboratory, Washington, DC 20375;
avourlid@pythia.nrl.navy.mil
Received 2001 November 21; accepted 2001 December 28

ABSTRACT

In an effort to understand what an "EIT wave" is and what its causes are, we have looked for correlations between the initiation of EIT waves and the occurrence of other solar phenomena. An EIT wave is a coronal disturbance, typically appearing as a diffuse brightening propagating across the Sun. A catalog of EIT waves, covering the period from 1997 March through 1998 June, was used in this study. For each EIT wave, the catalog gives the heliographic location and a rating for each wave, where the rating is determined by the reliability of the observations. Since EIT waves are transient, coronal phenomena, we have looked for correlations with other transient, coronal phenomena: X-ray flares, coronal mass ejections (CMEs), and metric type II radio bursts. An unambiguous correlation between EIT waves and CMEs has been found. The correlation of EIT waves with flares is significantly weaker, and EIT waves frequently are not accompanied by radio bursts. To search for trends in the data, proxies for each of these transient phenomena are examined. We also use the accumulated data to show the robustness of the catalog and to reveal biases that must be accounted for in this study.

Subject heading: Sun: activity — Sun: coronal mass ejections (CMEs) — Sun: flares — Sun: radio radiation — Sun: UV radiation — waves

1. INTRODUCTION

Since the discovery of "EIT waves" (Thompson et al. 1999), it has been suggested that they may be a coronal counterpart of Moreton waves. Moreton waves are observed in Hα images to propagate through the chromosphere away from the site of active region transients. They have long been thought to be initiated by a solar flare (Moreton 1961; Athay & Moreton 1961; Uchida 1968; Smith & Harvey 1971). Moreton waves have been observed to travel at a wide range of speeds, from 330 to 4200 km s^{-1} (Smith & Harvey 1971). EIT waves are large-scale coronal transients first observed with the Extreme Ultraviolet Imaging Telescope (EIT) on board the *Solar and Heliospheric Observatory* (*SOHO*; Delaboudinière et al. 1995; Domingo, Fleck, & Poland 1995). They appear as propagating EUV emission fronts, spreading outward from the site of active region transients at speeds of a few hundred kilometers per second. This general description roughly matches that of Moreton waves, and it is thus reasonable to assume that there may be some connection between Moreton and EIT waves. Moreton waves have been modeled by Uchida (1968, 1974) as a fast-mode MHD wave, and additional modeling has shown this description may work equally well or better for EIT waves (Wang 2000; Wu et al. 2001). There have been two instances of EIT waves and Hα Moreton waves observed in coincidence, and in both cases the waves developed cotemporally and cospatially (Thompson et al. 2000; Pohjolainen et al. 2001). Since Moreton waves are strongly associated with solar flares, if one can directly relate EIT waves to flares, it may be easier to draw the conclusion that an EIT wave is, or is not, in fact the coronal component of a Moreton wave.

A large number of EIT waves have now been observed; thus, reasonable attempts to conduct statistical studies can be done. Earlier studies of EIT waves have examined only a small number of cases. Thompson et al. (1999) presented the case of an EIT wave that occurred on 1997 April 7. This wave occurred in conjunction with an X-ray flare, a coronal mass ejection (CME), and a metric type II radio burst. Two cases occurring on 1997 September 24, presented by Thompson et al. (2000), had associated metric type II events and X-ray flares, but only one had an associated CME. Torsti et al. (1999) and Krucker et al. (1999) have investigated the relationship between EIT waves and interplanetary particle events. Both found in situ energetic populations of particles that seemed to be correlated with EIT waves crossing the coronal region magnetically connected to the in situ observations.

One previous study has attempted to relate EIT waves with other solar phenomena. Klassen et al. (2000) used a list of metric type II events observed in 1997 with the Potsdam radio spectral polarimeter to look for an association with EIT waves. Of the 21 Potsdam type II events, 19 (or 90%) were found to have associated EIT waves. There was no correlation found between EIT-wave speed and type II speed.

TABLE 1
Wave Classification

Rating	Description	Confidence Level (%)
Q0.....	Not likely to be a wave/poor data coverage	<10
Q1.....	Faint appearance, still unclear	<25
Q2.....	Propagation of brightened front	>25
Q3.....	Propagation of brightened front	>50
Q4.....	Almost definitely	>75
Q5.....	Clear propagation of front	~100

The Klassen et al. (2000) work was the primary motivation for the study presented here. The difficulty with interpreting the Klassen et al. (2000) results in light of EIT waves is that it is not clear what percentage of EIT waves have associated type II radio events. Rather, it is only known what percentage of type II radio bursts have associated EIT waves. This study begins with a comprehensive catalog of EIT waves and searches for associated phenomenon, whereas Klassen et al. (2000) selected events based on a list of metric type II events.

2. THE EIT DATA

The EIT-wave catalog used in this study encompasses 173 EIT waves observed from 1997 March through 1998 June (D. C. Myers & B. J. Thompson 2002, in preparation). The catalog was compiled by examining all EIT 195 Å (Fe XII) images from the start of the period when EIT began regularly taking images at a sufficient cadence to observe EIT waves (1997 March 24). This corresponds to an image cadence that is typically faster than 20 minutes. The catalog ends at the time of the interruption of the *SOHO* mission in 1998 June. Each wave is classified by a quality rating, which is described in Table 1, from Q0 to Q5. The quality rating describes the confidence level that the transient event observed is really an EIT wave. For example, cases with a rating of Q0 were typically events that were extremely weak or had poor data coverage. It may be possible that a number of events that received low quality ratings do not have the physical properties of an EIT wave at all and are transient brightenings due to an entirely different process. A Q5 rating refers to those transients that were well defined and clearly visible in the data. Note that this classification scheme is not equivalent to the intensity or speed of a wave. However, the visibility of a wave, and thus its quality rating, is likely to depend on these to at least some extent. Also listed in the catalog is the heliographic location of the assumed origin of each EIT wave. A more detailed description of these ratings and of the full catalog can be found in the catalog of Myers & Thompson.

Most of the EIT waves reported in the Myers & Thompson catalog consist of diffuse brightenings of relatively low amplitude. However, a very small fraction of the EIT waves (7%) had sharp, bright components associated with them. The majority of the observations of sharp waves, which are designated with an "S" in their rating (e.g., Q4S), also show the more typical diffuse brightenings. An example of an EIT wave from 1997 September 24 that exhibits both diffuse and sharp features is shown in Figure 1, which is adapted from Thompson et al. (2000). The first three panels show EIT images from 02:49, 03:03, and 03:23 UT with a pre-event image from 02:32 UT digitally differenced from them. Arrows indicate the progress of the EIT-wave front(s), though the front is faint by the third image and only an approximate location is indicated. The fourth panel shows a subfield of the first (undifferenced) image, illustrating the sharp brightening as it appeared in the 02:49 image. There is no evidence of a sharp brightening in subsequent images, though the diffuse wave fronts continue to be visible.

Because of the relatively poor temporal cadence of EIT, it is difficult to determine the exact start time or origin of the EIT waves. Given in the catalog is the time of the first image in which each wave is visible and also the time of the last image prior to the wave. It is generally assumed that the EIT waves were initiated in this interval or only slightly prior to it. In the example in Figure 1, the start time of the wave is assumed to be between 02:32 and 02:49 UT. The location of the origin of the wave is determined by the position of the active region from which the EIT wave apparently emanates. Because of the poor cadence, it is difficult to obtain reliable speeds for many of the waves in the catalog, and thus wave speeds are not considered here.

3. OTHER DATA

3.1. *Solar Flares*

NOAA *GOES* 3 s X-ray monitor data were used to identify solar flares. These data were used since the *GOES* instruments observe the Sun continuously, resulting in a good overlap in coverage with *SOHO*. In this study, a solar flare is defined as any significant, impulsive, transient increase in X-ray flux. Given the time of the first EIT image with a wave visible and the time of the last image prior to

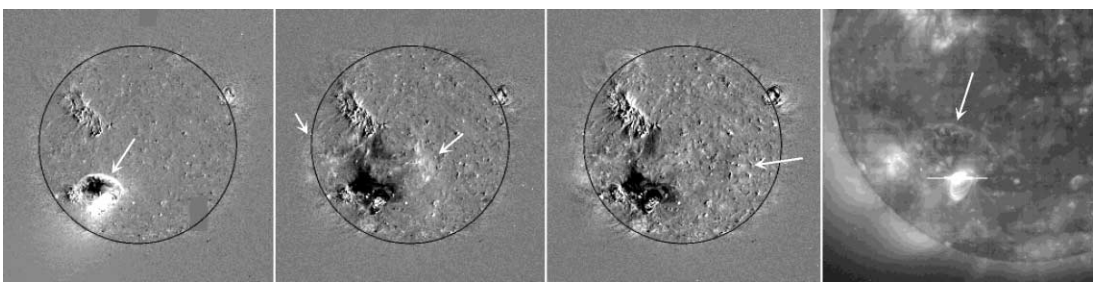

FIG. 1.—Example of an EIT wave from 1997 September 24. The first three panels show successive EIT images at 02:49, 03:03, and 03:23 UT with a pre-event image digitally differenced from them. Arrows indicate the EIT-wave front(s). The last panel shows a subfield of the first panel (undifferenced), showing an example of a sharp brightening.

the wave, the *GOES* data were searched for flares coincident with the given time interval. After an initial survey of the data, it became clear that the initial rise of the *GOES* event was more likely to occur in the given time interval whereas the peak in the *GOES* event could occur in the interval or even well after the wave was first visible on the disk. Thus, for an X-ray event to be considered associated with an EIT wave, the start of the rise in X-rays had to occur in the interval between the last EIT image prior to the wave and the first image with a wave visible. Occasionally, there were cases where ambiguities existed, such as nearly simultaneous X-ray flares. In these cases, wherever possible, Hα observation reports were used to verify the origins of the simultaneous events. In cases where ambiguities still remained, those waves were not included in the statistical results presented in this paper. In addition to determining the start and peak time of the X-ray event, the peak and background flux values were recorded.

3.2. *Coronal Mass Ejections*

The Large Angle Spectrometric Coronagraph (LASCO) on board *SOHO* was used to determine whether a CME occurred in association with each EIT wave. LASCO is a three-coronagraph package (C1, C2, and C3) that images the solar corona from apparent heliocentric distances of 1.1–30 $R_\odot$ (Brueckner et al. 1995). LASCO was used for CME identification because it generally observes the Sun at the same times as EIT. The C2 coronagraph was used in this study because of its relatively good cadence ($\sim$20 minutes) and because it is a white-light coronagraph. Because a basic component of CMEs is a density enhancement, white-light coronagraphs are ideal for observing them via Thomson-scattered photospheric light. The C2 field of view (2.5–6 $R_\odot$) allows a better determination of the start time of the CME than the C3 coronagraph, which has a 4–30 $R_\odot$ field of view. To determine whether or not there was a coronal mass ejection associated with the wave, running difference movies were closely examined around the time of the wave. Typically, the associated CMEs found were first visible in LASCO C2 within $\sim$2 hr of the time the EIT wave was first seen in EIT. Such a close temporal coincidence was generally enough to unambiguously identify the CME associated with a particular wave, since the data from this study are from the early phase of the solar cycle, when activity is lower. In addition to the close temporal association, the location of the EIT wave on the solar disk and the location of the LASCO CME were required to be consistent. For example, if an EIT wave occurred near the east solar limb, only a CME that was also observed on the east limb would be considered to be associated. For each event, the time the CME first appeared in C2 was recorded. Also, an on-line (Internet) list compiled by O. C. St. Cyr was used to obtain the CME speeds,[1] though speeds were not available for all CMEs.

3.3. *Type II Radio Bursts*

The radio type II observations used in this study were obtained from the various observatories that report events in the Solar Geophysical Data (SGD) "Yellow Books." Some additional events were found in a separate list maintained by the Potsdam Radio Observatory.

The SGD list of events was examined for any type II radio bursts around the time of the wave. As with the other associated phenomena, a temporal coincidence was required. A typical type II burst associated with the EIT wave would begin between the time of the EIT image prior to the wave and the time of the image showing the wave. Occasionally, the type II burst would begin shortly after the wave was already visible in EIT.

For the cases where no type II burst was reported, it was necessary to determine whether this was because there was truly no event or whether no observatories were operating at the time of the EIT wave. If there was no report of a type II burst and it was impossible to determine whether at least one radio observatory with metric coverage (in the range of 25–500 MHz) was operating, then that particular event would not be included in the statistical calculations. The SGD books reported observing times for certain observatories. For other observatories, it was assumed that they were observing only if they reported some other type of radio event at or near the time a type II burst was expected.

In addition, the Hiraiso Radio Spectrograph (HiRAS) dynamic spectrum plots were examined visually when no type II event was reported at the time of an EIT wave. HiRAS observations were typically available between 22 and 7 UT. This check of the Hiraiso data did not reveal any additional events. In two cases, there was a CME on one limb and an EIT wave on the opposite limb, and Nançay Radioheliograph data were used to verify that the type II burst was associated with the CME and not the EIT wave.

Reported speeds of type II bursts are not used here. Comparing speeds from different observatories is difficult since the derived speeds depend on the particular density model used. Individual observatories use different density models, resulting in some discrepancies in the reported speeds.

4. ANALYSIS

Table 2 shows the fraction of waves that have associated flares, CMEs, and metric type II bursts. Events where ambiguities exist in determining whether there is associated emission are not included in Table 2. It is seen that there is no definitive correlation between EIT waves and any of the phenomena studied here. However, recalling that the EIT-wave classification system is not one of intensity or speed but rather confidence that the wave is a real wave, it makes sense to look at the statistics broken down according to wave classification. Doing this for all classes of EIT waves, it is seen in Table 2 that there is some correlation between

TABLE 2
WAVE ASSOCIATIONS

Class	Number of Waves	Flares (%)	CMEs (%)	Type II Events (%)
C0.....	36	58	39	12
C1.....	50	62	47	23
C2.....	39	72	71	22
C3.....	26	62	65	41
C4.....	17	82	81	69
C5.....	5	100	100	100
Total...	173	66	58	29

[1] Available at ftp://lasco6.nascom.nasa.gov/pub/lasco/status/Version2_CME_Lists.

the wave classification rating and the existence of associated events of all types. For example, only ~50% of Q0 waves had associated flare, CME, or type II radio events. However, for the five cases of Q5 waves, there was always a flare, CME, and type II radio burst. For three of the other classes (Q2–Q4), the waves had essentially equal numbers of associated flares and CMEs and a smaller fraction of associated type II events. On the basis of these statistics alone, one might believe that EIT waves are equally likely to be associated with flares and CMEs. However, systematic sorting of the data, as is done in the following section, reveals more information.

4.1. *Correcting for Visibility*

If one takes the classification system at face value, then it may not be unreasonable to believe that 18%–19% of the Q4 waves do not have associated flares or CMEs. After all, that percentage is consistent with the statement that Q4 waves are believed to be waves with a greater than 75% confidence level. An additional piece of information in the EIT-wave catalog is the approximate heliographic location of the wave initiation. Here, it is assumed that any associated phenomenon has an origin close to that same location. The location of an event on the Sun can very obviously affect the ability to detect the event. The following sections detail how the visibility of each type of associated phenomenon is affected and how it has been corrected.

4.1.1. *Flares*

The solar flare soft X-ray emission detected by *GOES* is emitted isotropically. However, the flare plasma emitting the soft X-rays can be very low in the corona or chromosphere. Thus, any flare that occurs on the far side of the Sun cannot be detected unless it is close to the solar limb. There are a large number of EIT waves described as having origins at or behind the solar limb. Because of uncertainties in determining which of these may have had their origin over the limb or how far over they occurred, waves which had central meridian distances (CMDs) of 90° were considered separately. Table 3 shows the percentage of EIT waves that had associated flares as a function of the wave rating, with limb events (CMD = 90°) and disk events (CMD < 90°) shown separately.

As might be expected, there is a poor correspondence between flares and EIT waves occurring at the limb. For disk events, there is, in general, a high rate of coincidence, but there is far from a perfect correspondence. Only for the highest classification of waves, the Q5 category, is there a one-to-one correlation. When lower rated categories are included, the coincidence goes down substantially. In order to ensure that there was no bias introduced by high soft X-ray background levels, the background rates were also recorded for each EIT wave. For example, there was a Q4-rated EIT wave that occurred at heliographic coordinates 26N, 6E before 13:29 UT on 1997 October 23. The *GOES* background flux at the time was at the A3 (3×10^8 W m^{-2}) level. There is no evidence for an impulsive increase in the *GOES* X-ray intensity at the time of the EIT wave. A disappearing filament corresponding to the EIT-wave location was reported by the Ramey AFB station, and there was some EUV brightening corresponding to the filament evolution.

For each EIT wave with an associated flare, the peak flux of the flares as a function of EIT-wave class has been plotted in Figure 2. Because of the large scatter, there is no statistically significant trend seen in these data. There is, however, a tendency for waves with a higher rating to be associated with larger flares.

4.1.2. *CMEs*

For CMEs, the visibility issue is more complex. White-light coronagraphs are strongly biased toward detecting density enhancements in the plane of the sky. A CME that occurs on the limb would have a higher probability of detection than a disk-center CME. Disk-center CMEs, which sometimes produce halo CMEs, generally need to be of higher mass or larger size to be detected (Howard et al. 1982; Webb et al. 2000). Thus, CMEs with an origin near disk center are separated from those with an origin near the limb. Shown in Figure 3 is a plot of the number of EIT waves and the number of associated CMEs as a function of central meridian distance. The percentage of EIT waves with associated CMEs increases with increasing CMD. A demarcation of 60° was chosen to separate limb and disk CMEs. A typical CME is assumed to be ≤50° in width (St. Cyr et al. 1999), and thus any CME within 30° of the limb is likely to have a component in or close to the plane of the sky. Table 3 shows the percentage of EIT waves, as a function of the rating, which had associated CMEs, separated into disk and limb events.

For EIT waves occurring within 60° of CMD, there is a very poor correspondence between waves and CMEs. How-

TABLE 3
WAVE ASSOCIATIONS ACCORDING TO LOCATION

	Flares				CMEs				Type II Radio Events			
	Disk Events		Limb Events		Longitude < 60°		Longitude > 60°		Midlatitude		Center and Limb	
Class	Number of Waves	Flares (%)	Number of Waves	Flares (%)	Number of Waves	CMEs (%)	Number of Waves	CMEs (%)	Number of Waves	Type II Events (%)	Number of Waves	Type II Events (%)
Q0.....	31	61	5	40	27	30	9	67	12	0	18	11
Q1.....	40	63	10	60	31	39	16	63	15	20	28	21
Q2.....	26	73	13	69	16	50	22	86	8	25	22	27
Q3.....	23	61	3	67	19	42	5	100	10	40	12	42
Q4.....	11	91	6	67	10	70	6	100	4	50	12	75
Q5.....	5	100	0	...	5	100	0	...	0	...	4	100

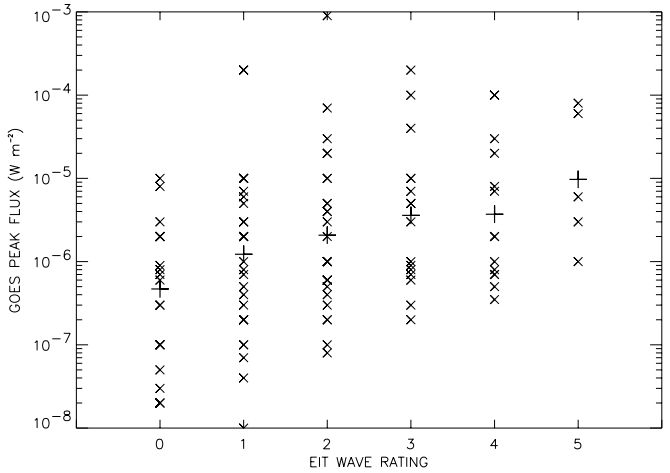

FIG. 2.—Peak *GOES* X-ray flux of each EIT-wave–associated flare as a function of the EIT-wave rating. The plus signs show the average flare size for each rating.

ever, when only EIT waves within 30° of the limb are examined, there is a dramatic correlation between the occurrence of CMEs and EIT waves. Note that there are no Q5-category events at the limb, but these may be considered a special case. Although there are only a few Q5-wave cases, they are all close to disk center, so it appears that there may be biases in the categorization of EIT waves, with a tendency to give higher ratings to disk-center events than to limb events. This is probably due to EIT waves having greater visibility on the solar disk, thereby affecting the quality rating. These revised statistics show that in fact all of the Q3 and Q4 EIT waves occurring near the limb also have CMEs. There are only 16 waves, of the total 173 studied, in this subset, but the result is nonetheless striking. Continuing down to the Q2-rated limb waves, 86% of them (19 of 22) had associated CMEs. As the definition of a Q2 wave means that some fraction of them may not even be real waves, this is a remarkable result. For the 38 highest rated limb EIT waves, 92% had an associated CME.

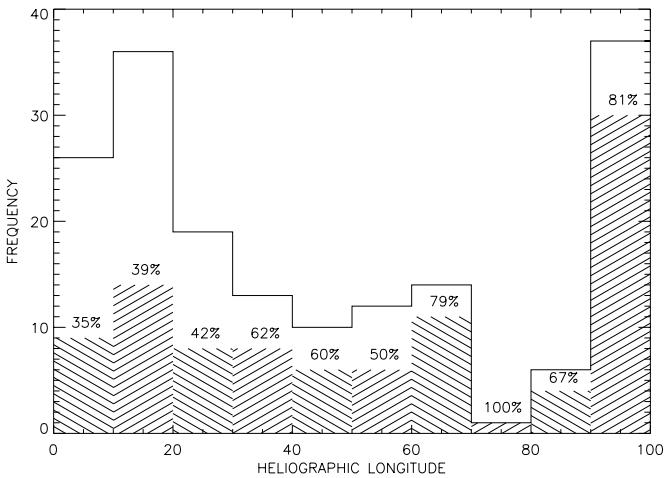

FIG. 3.—Number of EIT waves and CMEs as a function of heliographic longitude. The solid line indicates the number of EIT waves; the shaded area indicates the number of CMEs. The percentage of waves with associated CMEs is given.

Further inspection of the LASCO data for the three Q2-category waves that had no associated CME revealed that for two of those waves, there was generally a continuous outflow of material visible during the time of the EIT wave. There were no discrete ejections detected, but these may have been masked by the overall activity taking place. The corona was very quiet during the time of the third wave.

For the EIT waves with CMEs, the average CME speed as a function of wave class has been plotted in Figure 4. The CME speeds were taken from the on-line database of O. C. St. Cyr, where the CME speeds were given as the speed at the time of the last observation by LASCO. The speeds measured with LASCO are apparent speeds as projected onto the plane of the sky. Since CMEs typically propagate radially, at least within the LASCO field of view, a reasonable approach would be to compare the radial speed of CMEs, rather than plane-of-the-sky speed, to EIT-wave class. The correction from plane-of-the-sky speed to radial speed can be made knowing the heliographic coordinates of the source location, but without additional information it is model dependent. These data were corrected according to the model of Leblanc et al. (2002), which is similar to the 60° CME width case of the model of Hundhausen, Burkepile, & St. Cyr (1994). Figure 4 shows a trend, though not statistically significant, for increasing CME speed with increasing EIT-wave classification. Since speeds were not available for all of the CMEs, it is possible that there is some bias in the data, though there is no obvious reason to expect this.

4.1.3. *Metric Type II Events*

The ability to detect type II bursts is also sensitive to the plane-of-the-sky angle. Type II events on the disk are frequently seen in both the fundamental plasma frequency and in the first harmonic, while at the limb usually only the harmonic is detected. Thus, in general, type II events can be seen regardless of their longitude. However, it has been shown by Švestka & Fritzová-Švestková (1974) that the detection rate of type II events as a function of CMD shows lower rates at both disk center and at the limb, with a higher rate near CMDs of 30°–40°. In a study of 166 events, they found that the type II event rate at disk center and at the limb were approximately 40% lower than at midlongitudes.

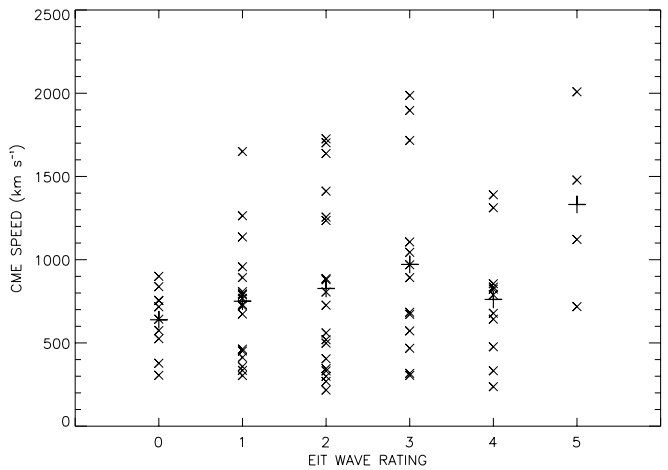

FIG. 4.—Speed of each EIT-wave–associated CME as a function of the EIT-wave rating. The speeds have been corrected for the plane-of-the-sky angle. The plus signs show the average CME speed for each rating.

Thus, it appears that many type II events occurring at disk center and the limb are not detected. Therefore, these data are also divided into two groups. The first group is events with CMDs between 22°.5 and 67°.5, and the second group of events comes from two bands: 0°–22°.5 and 67°.5–90°. Given the result of Švestka & Fritzová-Švestková (1974), one would expect that the first group would have the highest visibility.

Table 3 shows that there is a stronger correlation between EIT waves and type II events for the events at disk center and the limb than for events at an intermediate longitude. However, the overall percentages are relatively low. If only the wave-class Q3–Q5 events are included, the percentage of waves at intermediate longitudes with type II events is 43% and the percentage of waves at disk center and the limb with type II events is 64%. The results of Švestka & Fritzová-Švestková (1974) indicate that disk-center and limb type II events are undercounted, so the percentage of waves in that group with type II events may be higher.

4.2. "*S*"-Rated EIT Waves

Given the number of observations of EIT waves with sharp brightenings, they appear to be a very small subclass. However, the two cases where EIT waves and Hα Moreton waves have been correlated fall into this category (Thompson et al. 2000; Pohjolainen et al. 2001), so here the events with sharp brightenings are singled out for correlation with CMEs, flares, and type II bursts.

Table 4 lists the results of this analysis. Of the 12 EIT waves with sharp brightenings, three did not have associated flares (two of these having a low rating of Q0S, the other being a Q2S wave at the limb). Most of the disk-center events and all the limb events had CMEs, while all but one of the events had an associated type II burst. The correlations of waves with sharp brightenings and other solar phenomena appear much stronger than the results listed in Table 3, with a similar effect when the events are divided according to observation longitude. It appears that the waves with sharp brightenings fit well with the statistics of the Q4 and Q5 diffuse waves; although the appearance of sharp brightenings did not influence the quality rating assigned an event, it may be reasonable that the observation of a sharp bright front can be used as a factor in increasing the quality rating of a wave.

5. DISCUSSION

In the previous section, it was demonstrated that there is a very strong correlation between EIT waves and coronal mass ejections. If an EIT wave is observed, there must be a CME; however, the converse is not necessarily true. This brings up the issue of whether the relationship is causal or not. One way to investigate this relationship would be to examine the initiation times and locations of the two types of events. Unfortunately, the initiation times of both EIT waves and CMEs, as well as the exact origin of their initiation, are fairly uncertain. In order to gain some insight into this, the velocity profiles of some of the CMEs have been examined. It has been suggested that there are two classes of CMEs that can be identified by their height-time (H-T) profiles (Sheeley et al. 1999; Andrews & Howard 2001). Some CMEs observed with LASCO have H-T profiles that show significant acceleration, while others show a constant velocity, which is usually very fast. It has been suggested that constant-velocity profiles are for flare-associated CMEs (impulsive CMEs) and acceleration profiles are for CMEs with no flare (gradual CMEs). Since we did not find a clear EIT-wave–and–flare relationship, we might expect the H-T plots from CMEs associated with EIT waves to fall into both classes. Inspection of the H-T profiles for the Q4- and Q5-category waves reveals profiles of both types, with the acceleration profiles matching up with the flareless CMEs and the constant-velocity profiles matching up with the flare-associated CMEs. The CME speeds are not necessarily very high, even in the cases of the impulsive CMEs. There are cases of limb EIT waves having associated CME H-T profiles with constant speeds of $\sim$300 km s^{-1}. Thus, there does not appear to be a need for impulsive, fast CMEs for there to also be an EIT wave.

This also has some bearing on the issue of whether EIT waves are related to Moreton waves. As stated earlier, it has long been thought that Moreton waves are associated with solar flares. However, there are clear cases of EIT waves originating near disk center with no associated flares. In two of the cases where the EIT waves had a sharp, bright feature associated with them, other studies have shown that there was a correlated Moreton wave. Thus, the sharp, bright feature, only occasionally seen in EIT waves, may be a signature of a Moreton wave. It may be that Moreton waves are just a special case of the EIT-wave phenomenon. It has been shown that the normal, diffuse EIT waves are always CME

TABLE 4
Sharp Brightening–Associated Waves

	Flares				CMEs				Type II Radio Events			
	Disk Events		Limb Events		Longitude < 60°		Longitude > 60°		Midlatitude		Center and Limb	
Class	Number of Waves	Flares (%)	Number of Waves	Flares (%)	Number of Waves	CMEs (%)	Number of Waves	CMEs (%)	Number of Waves	Type II Events (%)	Number of Waves	Type II Events (%)
C0.....	2	0	0	...	2	50	0	...	1	0	1	0
C1.....	0	...	0	...	0	...	0	...	0	...	0	...
C2.....	1	100	3	67	0	...	4	100	0	...	4	75
C3.....	4	100	0	...	3	100	1	100	0	...	4	100
C4.....	1	100	0	...	1	0	0	...	1	100	0	...
C5.....	1	100	0	...	1	100	0	...	1	100	0	...

associated and that most have associated flares, but the sharp EIT waves are always associated with both flares and CMEs. Thus, a solar flare may indeed be the important mechanism for the creation of a Moreton wave. Several authors (Thompson et al. 2000; Wang 2000) have indicated that some of the EIT waves may be an ordinary fast-mode MHD disturbance while other EIT waves may be associated with a super-Alfvénic shock. One might assume that the shock cases are those EIT waves with a sharp bright front, and if these do indeed correspond to Moreton waves, then the flare association may be necessary for the shock.

No obvious explanation is available for the poor correlation between EIT waves that occur at intermediate central meridian distances (22°.5–67°.5) and type II bursts. However, the relatively strong correlation between EIT waves at small and large longitudes and type II events would appear to be consistent with the results of Klassen et al. (2000). The relatively small number of correlated bursts in the higher rated categories may be giving a misleading result. Better statistics, i.e., more EIT waves, may give a different result. However, it is possible that additional criteria are necessary for the production of type II bursts and that EIT waves are a necessary but not a sufficient condition.

The correlations between the EIT-wave class and the peak flare flux and CME speed are generally very weak. If the correlations were done with EIT-wave speed or intensity, it may be that stronger correlations could be found.

6. CONCLUSIONS

This work used a catalog of 173 EIT waves to search for associated transient solar phenomena. The phenomena examined were solar flares observed in *GOES* soft X-ray channels, coronal mass ejections observed in *SOHO*/LASCO, and type II radio bursts reported by various ground-based observatories. It was found that in every case, having accounted for observational biases, a coronal mass ejection occurred in association with the EIT wave. Both flares and type II radio bursts occurred less frequently. This is in contradiction with the idea that EIT waves are related to Moreton waves, since Moreton waves are thought to be flare associated. However, a class of EIT waves that had sharp, bright features may be Moreton-wave associated. This class of EIT waves had associated flares and CMEs in every case. There was only a weak correlation found between EIT-wave rating and flare peak flux or CME speed. It is possible that comparisons between quantitative measures of EIT waves and quantitative measures of flares, CMEs, and type II radio bursts may strengthen the correlations.

REFERENCES

Andrews, M. D., & Howard, R. A. 2001, Space Sci. Rev., 95, 147
Athay, R. G., & Moreton, G. E. 1961, ApJ, 133, 935
Brueckner, G. E., et al. 1995, Sol. Phys., 162, 357
Delaboudinière, J.-P., et al. 1995, Sol. Phys., 162, 291
Domingo, V., Fleck, B., & Poland, A. I. 1995, Sol. Phys., 162, 1
Howard, R. A., Michels, D. J., Sheeley, N. R., Jr., & Koomen, M. J. 1982, ApJ, 263, L101
Hundhausen, A. J., Burkepile, J. T., & St. Cyr, O. C. 1994, J. Geophys. Res., 99, 6543
Klassen, A., Aurass, H., Mann, G., & Thompson, B. J. 2000, A&AS, 141, 357
Krucker, S., Larson, D., Lin, R., & Thompson, B. J. 1999, ApJ, 519, 864
Leblanc, Y., Dulk, G. A., Vourlidas, A., & Bougeret, J.-L. 2002, J. Geophys. Res., in press
Moreton, G. E. 1961, S&T, 21, 145
Pohjolainen, S., et al. 2001, ApJ, 556, 421
Sheeley, N. R., Jr., Walters, J. H., Wang, Y.-M., & Howard, R. A. 1999, J. Geophys. Res., 104, 24739
Smith, S. F., & Harvey, K. L. 1971, in Physics of the Solar Corona, ed. C. J. Macris et al. (Dordrecht: Reidel), 156
St. Cyr, O. C., Burkepile, J. T., Hundhausen, A. J., & Lecinski, A. R. 1999, J. Geophys. Res., 104, 12493
Švestka, Z., & Fritzová-Švestková, L. 1974, Sol. Phys., 36, 417
Thompson, B. J., Reynolds, B., Aurass, H., Gopalswamy, N., Gurman, J. B., Hudson, H. S., Martin, S. F., & St. Cyr, O. C. 2000, Sol. Phys., 193, 161
Thompson, B. J., et al. 1999, ApJ, 517, L151
Torsti, J., Kocharov, L. G., Teittinen, M., & Thompson, B. J. 1999, ApJ, 510, 460
Uchida, Y. 1968, Sol. Phys., 4, 30
———. 1974, Sol. Phys., 39, 431
Wang, Y.-M. 2000, ApJ, 543, L89
Webb, D. F., Cliver, E. W., Crooker, N. U., St. Cyr, O. C., & Thompson, B. J. 2000, J. Geophys. Res., 105, 7491
Wu, S. T., Zheng, H., Wang, S., Thompson, B. J., Plunkett, S. P., Zhao, X. P., & Dryer, M. 2001, J. Geophys. Res., 106, 25089